

OPTIMAL FISH HARVESTING FOR A POPULATION MODELED BY A NONLINEAR PARABOLIC PARTIAL DIFFERENTIAL EQUATION

MICHAEL R. KELLY JR.

Department of Mathematics, The Ohio State University, 231 W. 18th Avenue, Columbus, OH
43210

E-mail: kelly.1156@osu.edu

YULONG XING

Department of Mathematics, The University of California Riverside, Surge 202, 900 University
Ave., Riverside, CA 92521

E-mail: xingy@ucr.edu

SUZANNE LENHART

Department of Mathematics, The University of Tennessee, 235 Ayres Hall, 1403 Circle Drive,
Knoxville, TN 37996

E-mail: lenhart@math.utk.edu

ABSTRACT. As the human population continues to grow, there is a need for better management of our natural resources in order for our planet to be able to produce enough to sustain us. One important resource we must consider is marine fish populations. We use the tool of optimal control to investigate harvesting strategies for maximizing yield of a fish population in a heterogeneous, finite domain. We determine whether these solutions include no-take marine reserves as part of the optimal solution. The fishery stock is modeled using a nonlinear, parabolic partial differential equation with logistic growth, movement by diffusion and advection, and with Robin boundary conditions. The objective for the problem is to find the harvest rate that maximizes the discounted yield. Optimal harvesting strategies are found numerically.

KEY WORDS: Partial differential equations, optimal control theory, fisheries, harvesting.

1. Introduction. There is growing concern over natural resource management and how best to use resources to sustain the world's growing population. An important resource to consider is fisheries, which are a source of food for people across the globe. However, many marine populations are severely overfished (Hilborn [2012]). In addition to the overexploitation of fish stock, there are threats of habitat degradation and destruction, pollution, and climate change impacts affecting the world's oceans (Neubert [2003], Hilborn [2012]). Researchers must understand what is necessary for assuring a stable supply of fish under environmental stressors of various kinds, while also considering the impact of human behavior on the environment

Corresponding author. Michael R. Kelly, Jr.; Department of Mathematics, The Ohio State University, 231 W. 18th Avenue, Columbus, OH 43210 E-mail: kelly.1156@osu.edu

Received by the editors on 31st December 2014. Accepted 27th July 2015.

(Joshi et al. [2008]). This is a difficult task given the large variability associated with fishery ecosystems yet there is continual pressure to find methods for optimally solving these management problems.

There has been work investigating various ways to help restore fish populations and protect marine ecosystems, such as time-area closures, limiting the fishing season, as well as the implementation of catch quotas. Another way to help protect fish populations from overexploitation is the inclusion of no-take marine reserves. These reserves are categorized as areas of the ocean completely protected: removal or destruction of natural resources is prohibited (Hilborn [2012]). They offer protection for both marine fish populations and their ecosystems. The establishment of no-take reserves is beginning to receive more attention on the global scale. The total amount of ocean set as marine protected areas (MPAs) has risen by over 150% since 2003. However, only 1.17% of the marine area of the world is protected as MPAs and only a small portion of MPA coverage is designated as fully protected, no-take areas (Toropova et al. [2010]). This may be because marine reserves are a controversial fishery management tool. Some believe that no-take marine reserves actually reduce the yield (Walters and Martell [2004], Clark [2006]).

The spatial structure of a renewable natural resource is important to consider when determining management strategies. Spatial heterogeneity and dynamics can affect management outcomes. When spatial dynamics of a resource are ignored, management strategies generally produce suboptimal results (Herrera and Lenhart [2010]). There have been many approaches to modeling spatial dynamics. Early harvesting models involving bioeconomics and optimal yield were done using ordinary differential equations. Clark's work provided a foundation for using optimal control theory as a tool in fishery management (Clark [1985, 1990]).

Metapopulation models are a common spatial modeling approach, which divides the environment into a collection of patches. Tuck and Possingham used coupled spatially explicit difference equations to model a single-species, two-patch metapopulation. They considered the problem of optimally exploiting the single species local population that is connected by dispersing larvae to an unharvested second population (Tuck and Possingham [2000]). They showed that the closed areas had positive net benefits in terms of both stock abundance and economic rents. Sanchirico and Wilen studied a series of differential equation metapopulation models with logistic growth and density-dependent dispersal between patches coupled with a spatially explicit harvesting model (Sanchirico and Wilen [1999, 2001]). They investigated different scenarios, exploring the impacts of a reserve on biomass and effort distribution. Results showed that, under certain conditions, reserves increase both stock abundance and harvest effort (Sanchirico and Wilen [2001]). Brown and Roughgarden formulated an optimal control problem for maximizing the discounted profit, using a metapopulation ordinary differential equation (ODE) model (continuous in time, discrete in space) for an age-structured fish stock. Their results demonstrate that reserves can be part of the optimal solution (Brown and Roughgarden [1997]).

There have been studies that sought yield maximizing strategies without imposing no-take reserves in the model. Neubert investigated the steady states of a fish stock in a spatially explicit harvesting model, ignoring the dependence of the stock on time (Neubert [2003]). His model is a second-order ODE in space. The benefits of using a spatially explicit model include a more realistic marine reserve in a fixed area of space through which fish move, rather than a fixed harvesting rate across the domain. His objective functional sought to find the fishing effort that maximizes the yield. His model did not incorporate reserves into the model yet they were shown to be part of the resulting optimal harvesting strategy (depending on the length of domain). Neubert also found “chattering” in the optimal control in some cases, which are infinite sequences of reserves alternating with areas of intense fishing.

Ding and Lenhart [2009] extended Neubert’s work to a multidimensional spatial domain, considering different types of objective functionals. They sought to find an optimal fishery harvesting strategy with fish stock modeled by a semilinear elliptic partial differential equation (PDE) with Dirichlet boundary conditions. One of their objective functionals was similar to that of Neubert but considered the difference between the yield and a nonlinear cost. Ding and Lenhart [2009] also included the minimization of the variation in the control (with H^1 controls) to avoid “chattering.” Both functionals result in a reserve as part of the optimal harvesting strategy. De Leenheer also investigated a steady-state, parabolic PDE model, rewritten as a system of two first-order ODEs, to address the problem of where exactly to establish MPAs (De Leenheer [2014]). His objective involved maximizing fishing yield as well as fish densities. His results concluded that the location of the MPA was determined by the length of spatial domain and average fish density.

To include time-varying scenarios, Joshi et al. [2008] built a nonlinear parabolic PDE model for the growth, movement, and harvesting of a renewable resource. This work considered yield maximizing solutions, but in a dynamic fishery system, investigating the spatiotemporal distribution of harvesting effort and the existence of no-take marine reserves that arose as part of the harvesting strategy. Their nonsteady state equation also included an advection term. This work was concerned not only with the existence of reserves, but the time of their establishment and the evolution of its size over time.

The PDE models of Joshi et al. [2008], Ding and Lenhart [2009], Neubert [2003] for optimal fish harvesting had Dirichlet boundary conditions, representing a lethal domain boundary. This would occur if you had a habitat imbedded into a larger, uninhabitable region. Although many fisheries are not found in such conditions, the impact of alternative boundary conditions was not addressed. Most fisheries occur on open ocean where these artificial boundaries do not exist. The implementation of an alternative type of boundary condition, Robin boundary conditions, deemed more favorable to the fish stock, could produce an alternative optimal harvesting strategy.

Optimal control of parabolic PDEs with Robin boundary conditions has been successfully used for other applications. Previous work on these boundary conditions

was done by Lenhart and Wilson [1993] in investigating optimal control of a heat transfer equation with a convective boundary condition. There has also been work done with these boundary conditions in biological applications. Lenhart and collaborators [1999] considered a case with a boundary hostile to two interacting species, using Robin boundary conditions. For a detailed discussion about specific populations and the biological interpretation of such boundary conditions, see the paper by Fagan et al. [1999].

Modeling these dynamic systems can help predict the impact of fishing regulations. We formulate a model on a heterogenous, spatiotemporal domain with more realistic boundary conditions to represent the habitat and the fish movement and to gain important insights on optimal harvesting strategies. These models provide guidance to make decisions to improve marine resources without compromising the economic yield.

In the next section, we formulate the problem in an appropriate weak solution space and describe the spatiotemporal model for the fish stock and assumptions. We then prove existence and uniqueness of our state solution using an iteration scheme and *a priori* estimates. The proof for the existence of an optimal control is given. Next, we derive the optimality system consisting of the state system coupled with the adjoint system and an optimal control characterization. We prove the uniqueness of the optimality system, guaranteeing the uniqueness of the optimal control solution. Finally, we illustrate some examples by approximating our solutions using numerical methods, and give some conclusions.

2. Problem formulation. The focus of the project is on optimal harvesting strategies of a fish population in a heterogeneous, finite domain. We develop resource management strategies, specifically yield-maximizing solutions, and determine whether these solutions include no-take marine reserves as part of the optimal control.

The fishery stock is modeled using a nonlinear, parabolic partial differential equation with both diffusion and advection on a multidimensional, smooth, bounded domain $Q = \Omega \times (0, T)$ with Robin boundary conditions:

$$(1) \quad u_t = \sum_{i,j=1}^n (a_{ij}(x,t)u_{x_i})_{x_j} + \sum_{i=1}^n b_i(x,t)u_{x_i} + f(u) - h(x,t)u \quad \Omega \times (0, T),$$

$$(2) \quad \frac{\partial u}{\partial \nu}(x,t) + qu(x,t) = 0 \quad \partial\Omega \times (0, T),$$

and initial condition:

$$(3) \quad u(x, 0) = u_0(x) \quad x \in \Omega,$$

where $u(x, t)$ is the fish stock density. The conormal derivative is given by $\frac{\partial u}{\partial \nu} = \nabla_x u \cdot \nu$ with $\nu = (\nu_1, \dots, \nu_n)$ and $\nu_i = \sum_{j=1}^n a_{ij}(x, t)\eta_j$, with η_j being the outward normal unit vector. The nonlinear growth term is given by $f(u)$ and $h(x, t)$ is the harvest rate. The diffusion and advection coefficients are heterogenous functions and given by $a_{ij}(x, t)$ and $b_i(x, t)$, respectively. Also, the initial population $u_0(x) \in L^\infty(\Omega)$ is nonnegative. For this application, our spatial domain Ω is a smooth, bounded open set in \mathbb{R}^n , $n = 1, 2$, or 3 , although the theorems are true for multidimensional domains for any integer $n \geq 1$. The Robin boundary condition constant, q , is nonnegative.

Movement of the fish stock is modeled using diffusion and advection. Diffusion forces the stock to not congregate to one centralized area, while advection accounts for currents and drifts in the domain. Robin boundary conditions, where the flux at the boundary is proportional to the stock density at the boundary, are more favorable to the fish stock than Dirichlet boundary conditions, which represent a lethal domain surrounding our spatial domain. We investigate population dynamics with logistic growth. The goal for our problem will be to find the harvest rate, $h(x, t)$, that maximizes the discounted yield. Let P be the price constant, which we will set to $P = 1$, and think of the value of $J(h)$ as money. Let μ be the discount factor. The objective functional is

$$(4) \quad J(h) = \int_0^T \int_{\Omega} P e^{-\mu t} h u \, dx dt,$$

which is maximized over the set of admissible controls:

$$\mathcal{H} = \{h \in L^\infty(Q) : 0 \leq h(x, t) \leq h_{max}\}.$$

Given $h \in \mathcal{H}$, we denote by $u = u(h)$, the corresponding state solution, with the state u satisfying (1)–(3). We make the following assumptions:

- (i) Uniform ellipticity on the diffusion coefficient:
There exists $\theta > 0$ such that

$$\theta \sum_{i=1}^n \xi_i^2 \leq \sum_{i,j=1}^n a_{ij}(x, t) \xi_i \xi_j \quad \text{for all } (x, t) \in Q, \xi \in \mathcal{R}^n.$$

- (ii) Symmetry in the diffusion coefficients:

$$a_{ij} = a_{ji} \quad \text{for } i, j = 1, \dots, n.$$

(iii) Bounded coefficients:

$$a_{ij}, b_i \in C^1(\bar{Q}) \text{ for all } i, j = 1, \dots, n.$$

(iv) The growth term can be written as $f(u) = ug(u)$ where $g \in C^1(\mathbb{R})$ for all $u \geq 0$.

(v) There exists $r > 0$ such that $r \geq g(u)$ for all $u \geq 0$.

(vi) There exists $C_1 > 0$ such that for all $0 \leq u \leq M$, $g(u) \geq -C_1$.

(vii) There exists $C_2 > 0$ such that for all $0 \leq u \leq M$, $f'(u) \geq -C_2$.

(viii) The Robin boundary condition constant, q , is nonnegative.

(ix) The discount factor, μ , is a nonnegative constant.

(x) The initial condition $u_0 \in L^\infty$ and $0 \leq u_0 \leq K$ on Ω .

Remark 1. *Two examples of $f(u)$ functions that satisfy the above assumptions are*

$$f(u) = ru \left(1 - \frac{u}{K}\right),$$

where $r \geq 0$ is the growth rate and $K \geq 0$ is the carrying capacity of the population, and

$$f(u) = ru(1-u)(u-a),$$

with $0 < a < 1$.

3. Existence of an optimal control. The underlying solution space for our state system is given by $V \cap L^\infty(Q)$ where $V = L^2((0, T); H^1(\Omega))$ and the dual space for the time derivative of the solution is given by $V^* = L^2((0, T); H^1(\Omega)^*)$. Since $u \in V$ and $u_t \in V^*$, due to the results of Evans [2010],

$$u \in C([0, T]; L^2(\Omega)),$$

and the initial condition makes sense in $L^2(\Omega)$.

We first show *a priori* estimates that are needed for existence and positivity of the state solution.

Theorem 1. *Suppose $u \in V \cap L^\infty(Q)$ with $u_t \in V^*$ and $\|u\|_{L^\infty(Q)} \leq B$, is a weak solution of (1)–(3) corresponding to control $h \in \mathcal{H}$, and $u \geq 0$ a.e. in Q . Then there exists positive constants, K_1 , K_2 , and K_3 , such that*

$$(5) \quad \|u(h)\|_V \leq K_1,$$

$$(6) \quad \|(u(h))_t\|_{V^*} \leq K_2,$$

$$(7) \quad \int_{\partial\Omega \times (0,T)} u^2 \, dsdt \leq K_3,$$

with these bounds K_1, K_2, K_3 holding for all such state solutions.

Proof. Using u as the test function in the weak formulation on $Q_s = \Omega \times (0, s)$:

$$(8) \quad \begin{aligned} & \int_{(0,s)} \langle u_t, u \rangle \, dt + \int_{Q_s} \sum_{i,j=1}^n a_{ij}(x,t) u_{x_i} u_{x_j} \, dxdt + \int_{\partial\Omega \times (0,s)} qu^2 \, dsdt \\ &= \int_{Q_s} (f(u) - hu)u \, dxdt + \int_{Q_s} \sum_{i=1}^n b_i(x,t) u_{x_i} u \, dxdt. \end{aligned}$$

Using $hu^2 \geq 0$ and uniform ellipticity on the diffusion coefficients, we have the following:

$$\begin{aligned} & \int_{(0,s)} \langle u_t, u \rangle \, dt + \theta \int_{Q_s} \sum_{i=1}^n (u_{x_i})^2 \, dxdt + \int_{\partial\Omega \times (0,s)} qu^2 \, dsdt \\ & \leq \int_{Q_s} f(u)u \, dxdt + \int_{Q_s} \sum_{i=1}^n b_i(x,t) u_{x_i} u \, dxdt. \end{aligned}$$

This equation, combined with the fact that

$$\frac{1}{2} \int_{Q_s} \frac{d}{dt} u^2 \, dxdt = \frac{1}{2} \int_{\Omega \times \{s\}} u^2(x, s) \, dx - \frac{1}{2} \int_{\Omega \times \{0\}} u^2(x, 0) \, dx$$

gives

$$\begin{aligned} & \frac{1}{2} \int_{\Omega \times \{s\}} u^2(x, s) \, dx + \theta \int_{Q_s} \sum_{i=1}^n (u_{x_i})^2 \, dxdt + \int_{\partial\Omega \times (0,s)} qu^2 \, dsdt \\ & \leq \int_{Q_s} f(u)u \, dxdt + \int_{Q_s} \sum_{i=1}^n b_i(x,t) u_{x_i} u \, dxdt + \frac{1}{2} \int_{\Omega} u_0^2(x) \, dx. \end{aligned}$$

Using Cauchy's Inequality on the b_i terms, multiplying by 2, and collecting u_{x_i} terms on the LHS, the structure assumptions (2) and (2) on $f(u)$ give

$$(9) \quad \int_{\Omega \times \{s\}} u^2(x, s) dx + 2\theta \int_{Q_s} \sum_{i=1}^n (u_{x_i})^2 dxdt + 2 \int_{\partial\Omega \times (0, T)} qu^2 dsdt \\ \leq 2(r + C_{\theta, b}) \int_{Q_s} u^2 dxdt + \int_{\Omega} u_0^2(x) dx.$$

Using $q \geq 0$ and Gronwall's Inequality, we have

$$\int_{\Omega \times \{s\}} u^2(x, s) dx \leq 2(r + C_{\theta, b}) \int_{Q_s} u^2 dxdt + \int_{\Omega} u_0^2(x) dx,$$

so that

$$\int_{\Omega \times \{s\}} u^2(x, s) dx \leq \|u_0\|_{L^2(\Omega)}^2 (1 + G_1 e^{G_1 s}),$$

where $G_1 = 2(r + C_{\theta, b})$. Taking the maximum over time, we obtain the following:

$$(10) \quad \max_{0 \leq t \leq T} \|u(\cdot, t)\|_{L^2(\Omega)}^2 \leq \|u_0\|_{L^2(\Omega)}^2 (1 + G_1 e^{G_1 T}).$$

Using $\hat{G} = \|u_0\|_{L^2(\Omega)}^2 (1 + G_1 e^{G_1 T})$ in (9), we have

$$(11) \quad \theta \int_Q \sum_{i=1}^n (u_{x_i})^2 dxdt + 2 \int_{\partial\Omega \times (0, T)} qu^2 dsdt \leq 2T(r + C_{\theta, b})\hat{G} + \int_{\Omega} u_0^2(x) dx.$$

Combining (10) and (11) gives the estimate of $\|u(h)\|_V$ and estimate (7). For the time-derivative estimate, we start with the PDE

$$u_t = f(u) - hu + \sum_{i,j=1}^n (a_{ij}(x, t)u_{x_i})_{x_j} + \sum_{i=1}^n b_i(x, t)u_{x_i}.$$

By the previous estimate, the right-hand side of the PDE is bounded in $L^2((0, T); H^1(\Omega)^*)$. Given our assumptions on $f(u)$, every term on the right-hand side is in L^2 or is the derivative of an L^2 function, thus we have the right-hand side of the PDE bounded in the dual space, which implies (6). \square

To carefully formulate our problem, we first must prove the existence of a state solution.

Theorem 2. *Given a control $h \in \mathcal{H}$, there exists a unique, weak solution, to (1)–(3) satisfying*

$$(12) \quad 0 \leq u(x, t) \leq B$$

and this bound, B , holds for all state solutions.

Proof. We will summarize the use of an iterative method and maximum principle arguments. First, we define U as a solution of the problem:

$$(13) \quad U_t - \sum_{i,j=1}^n (a_{ij}(x, t)U_{x_i})_{x_j} - \sum_{i=1}^n b_i(x, t)U_{x_i} = rU \quad \Omega \times (0, T),$$

$$(14) \quad \frac{\partial U}{\partial \nu}(x, t) + qU(x, t) = 0 \quad \partial\Omega \times (0, T),$$

$$(15) \quad U(x, 0) = u_0(x) \quad x \in \Omega.$$

Then this supersolution U is nonnegative and L^∞ bounded by construction. Then building the iteration scheme (Lieberman [1996], Evans [2010]), starting with $u^1 = U$, there exists a weak solution u^i for $i = 2, 3, \dots$ such that

$$u_t^i - \sum_{i,j=1}^n (a_{ij}(x, t)u_{x_i}^i)_{x_j} - \sum_{i=1}^n b_i(x, t)u_{x_i}^i + Ru^i = G(u^{i-1})$$

with the boundary and initial conditions (2) and (3), where $R > h_{max} + C_1 + C_2$, C_1, C_2 are the bounds from assumptions on f and $G(u^{i-1}) = Ru^{i-1} + f(u^{i-1}) - hu^{i-1}$.

We can show by induction, $0 \leq u^i \leq U$. We then can show that the state sequence has a monotone property, i.e., $u^{i+1} \leq u^i$, by an additional induction argument. Finally, using the *a priori* bounds from Theorem 1 on u^i and the monotone property, we have weak convergence on the sequences (not just on subsequences). There also exists $u^* \in V$ such that:

$$(16) \quad u^n \rightharpoonup u^* \quad \text{weakly in } V = L^2((0, T); H^1(\Omega)),$$

$$(17) \quad u^n \rightharpoonup u^* \quad \text{weakly in } L^2((0, T), L^2(\partial\Omega)),$$

$$(18) \quad u_t^n \rightharpoonup u_t^* \quad \text{weakly in } V^* = L^2((0, T); H^1(\Omega)^*).$$

Since $u \notin H^1(Q)$ and u_{x_i} and u_t have different regularity, by a result (Corollary 4) in Simon [1987]:

$$(19) \quad u^n \rightarrow u^* \text{ strongly in } L^2(Q).$$

We need this strong convergence in the terms with $f(u^i)$. By passing the limit in the weak formulation of the PDE, we conclude that u is a weak solution of (1)–(3). We then show that the state solution is unique using similar methods as in the proof of Theorem 1. \square

We denote the state solution corresponding to h as $u(h)$. Having existence, uniqueness, and estimates for our state solution, we will now prove the existence of an optimal control for our problem.

Theorem 3. *There exists an optimal control, $h^* \in \mathcal{H}$, satisfying*

$$J(h^*) = \sup_{h \in \mathcal{H}} J(h).$$

Proof. Note, from estimates (5) and (6), $\sup_{h \in \mathcal{H}} J(h)$ is finite. We can choose a maximizing sequence, $\{h^n\}$ in \mathcal{H} such that

$$\lim_{n \rightarrow \infty} J(h^n) = \sup_{h \in \mathcal{H}} J(h).$$

By the *a priori* estimates (5)–(7), there also exists functions $h^* \in \mathcal{H}$ and $u^* \in V \cap L^\infty(Q)$ such that, on a subsequence:

$$(20) \quad h^n \rightharpoonup h^* \text{ weakly in } L^2(Q),$$

$$(21) \quad u^n \rightharpoonup u^* \text{ weakly in } V = L^2((0, T); H^1(\Omega)),$$

$$(22) \quad u^n \rightharpoonup u^* \text{ weakly in } L^2((0, T), L^2(\partial\Omega)),$$

$$(23) \quad u_t^n \rightharpoonup u_t^* \text{ weakly in } V^* = L^2((0, T); H^1(\Omega)^*).$$

Again by a result in Simon [1987], we have:

$$(24) \quad u^n \rightarrow u^* \text{ strongly in } L^2(Q).$$

We now need to show that $u^* = u(h^*)$. We will use the fact that we have L^∞ bounds on the controls and corresponding states. We have the PDE (1) for the

subsequence, u^n :

$$(25) \quad u_t^n = f(u^n) - h^n(x, t)u^n + \sum_{i,j=1}^n (a_{ij}(x, t)u_{x_i}^n)_{x_j} + \sum_{i=1}^n b_i(x, t)u_{x_i}^n.$$

We will show that each term in the PDE for u^n and h^n converges to the corresponding term with u^* and h^* .

- (i) By assumption that the diffusion and advection coefficients are bounded, the weak convergence from (21) gives the convergence of those terms.
- (ii) By (24), we know u^n converges on a subsequence pointwise a.e. Since f is continuous, we have $f(u^n) \rightarrow f(u^*)$ pointwise. Thus,

$$\int_Q (f(u^n) - f(u^*))\phi \, dxdt \rightarrow 0.$$

- (iii) Using the weak convergence, (22), with $q\phi \in L^2(\partial\Omega \times (0, T))$, leads to

$$\left| \int_{\partial\Omega \times (0, T)} q(u^n - u^*)\phi \, dsdt \right| \rightarrow 0.$$

- (iv) By assumptions, we know the h^n sequence and u^* are bounded in L^∞ and

$$(26) \quad \begin{aligned} \left| \int_Q (h^n u^n \phi - h^* u^* \phi) \, dxdt \right| &= \left| \int_Q (h^n u^n \phi + h^n u^* \phi - h^n u^* \phi - h^* u^* \phi) \, dxdt \right| \\ &\leq \left| \int_Q (h^n (u^n - u^*) \phi) \, dxdt \right| + \left| \int_Q (h^n - h^*) u^* \phi \, dxdt \right| \\ &\leq \int_Q |h^n| |u^n - u^*| |\phi| \, dxdt + \left| \int_Q (h^n - h^*) u^* \phi \, dxdt \right|. \end{aligned}$$

For the first term in (26), the convergence (24) and Cauchy's Inequality give

$$\int_Q |h^n| |u^n - u^*| |\phi| \, dxdt \leq C \left(\int_Q |u^n - u^*|^2 \, dxdt \right)^{1/2} \left(\int_Q \phi^2 \, dxdt \right)^{1/2} \rightarrow 0.$$

For the second term, since u^* is bounded in L^∞ by results above, the product $u^* \phi \in L^2(Q)$. The weak convergence of $\{h^n\}$ gives

$$\left| \int_Q (h^n - h^*) u^* \phi \, dxdt \right| \rightarrow 0.$$

Using the above results, we conclude that

$$u^* = u(h^*).$$

By our choice of maximizing sequence, we have

$$\sup_h J(h) = \lim_{n \rightarrow \infty} J(h^n) = \lim_{n \rightarrow \infty} \int_0^T \int_{\Omega} e^{-\mu t} h^n u^n \, dx dt = J(h^*),$$

and hence h^* is an optimal control. \square

4. Derivation of the optimality system. Next, we derive the optimality system which consists of the state system coupled with the adjoint system and an optimal control characterization. We will need to differentiate the map $h \rightarrow J(h)$ to obtain our control characterization. Since u is involved in $J(h)$, we first differentiate the map $h \rightarrow u$.

Theorem 4. *Let h^* be an optimal control with corresponding state, u^* , and $h^\epsilon = h^* + \epsilon l$ be another control, where $\epsilon > 0$ and $l \in L^\infty(Q)$ is a variation function. The mapping $h \rightarrow u(h) \in V$ is weakly differentiable in the directional derivative sense: $\exists \psi \in V$ and $\psi_t \in V^*$ such that*

$$\lim_{\epsilon \rightarrow 0^+} \frac{u(h^* + \epsilon l) - u(h^*)}{\epsilon} = \psi(x, t)$$

weakly in V for any $h \in \mathcal{H}$. Then the sensitivity function ψ corresponding to the control satisfies:

$$(27) \quad \psi_t = f'(u^*)\psi - h^*\psi + \sum_{i,j=1}^n (a_{ij}(x, t)\psi_{x_i})_{x_j} + \sum_{i=1}^n b_i(x, t)\psi_{x_i} - lu^* \quad \Omega \times (0, T),$$

$$(28) \quad \frac{\partial \psi}{\partial \nu} + q\psi = 0 \quad \partial\Omega \times (0, T),$$

$$(29) \quad \psi(x, 0) = 0 \quad \Omega \times \{t = 0\}.$$

Proof. Let $u^\epsilon = u(h^\epsilon)$ where $h^\epsilon = h^* + \epsilon l$ and $u^* = u(h^*)$ where h^* is an optimal control, with the corresponding PDEs

$$(30) \quad u_t^\epsilon = f(u^\epsilon) - (h^* + \epsilon l)u^\epsilon + \sum_{i,j=1}^n (a_{ij}(x, t)u_{x_i}^\epsilon)_{x_j} + \sum_{i=1}^n b_i(x, t)u_{x_i}^\epsilon,$$

$$(31) \quad u_t^* = f(u^*) - h^* u^* + \sum_{i,j=1}^n (a_{ij}(x,t) u_{x_i}^*)_{x_j} + \sum_{i=1}^n b_i(x,t) u_{x_i}^*.$$

Subtracting (31) from (30) and dividing by ϵ , we get

$$\begin{aligned} \frac{u_t^\epsilon - u_t^*}{\epsilon} &= \frac{f(u^\epsilon) - f(u^*)}{\epsilon} - h^* \left(\frac{u^\epsilon - u^*}{\epsilon} \right) + \sum_{i,j=1}^n \left(a_{ij}(x,t) \left(\frac{u_{x_i}^\epsilon - u_{x_i}^*}{\epsilon} \right) \right)_{x_j} \\ &\quad + \sum_{i=1}^n b_i(x,t) \left(\frac{u_{x_i}^\epsilon - u_{x_i}^*}{\epsilon} \right) - \frac{\epsilon l u^\epsilon}{\epsilon}. \end{aligned}$$

By the techniques of Theorem 1 applied to the difference quotient in Theorem 4, we have boundedness of the difference quotients, the existence of ψ , and the corresponding convergence of difference quotients. For the nonlinear term, we see that, as $\epsilon \rightarrow 0$,

$$\frac{f(u^\epsilon) - f(u^*)}{\epsilon} = \frac{f(u^\epsilon) - f(u^*)}{u^\epsilon - u^*} \frac{u^\epsilon - u^*}{\epsilon} \rightarrow f'(u^*) \psi$$

using the result that $u^\epsilon \rightarrow u^*$ in $L^2(Q)$. Thus, with the convergence of each of the above difference quotients, the sensitivity ψ satisfies (27)–(29) in the weak sense. \square

Next, we use our adjoint function to characterize our optimal control. We rewrite the sensitivity PDE (27) as

$$L\psi = -lu^*,$$

where L is the operator:

$$L\psi = \psi_t - f'(u^*)\psi - \sum_{i,j=1}^n (a_{ij}(x,t)\psi_{x_i})_{x_j} - \sum_{i=1}^n b_i(x,t)\psi_{x_i} + h^*\psi.$$

The adjoint operator L^* is related to the operator L by the following L^2 operator duality:

$$\langle \lambda, L\psi \rangle = \langle L^*\lambda, \psi \rangle$$

with

$$\langle v, w \rangle = \int_{\Omega} vw \, dxdt.$$

To use $L\psi$ to get an expression for $L^*\lambda$, the adjoint operator, formally we write

$$\int_0^T \int_{\Omega} e^{-\mu t} h^* \psi \, dx dt = \int_0^T \int_{\Omega} e^{-\mu t} L^* \lambda \psi \, dx dt = \int_0^T \int_{\Omega} e^{-\mu t} \lambda L \psi \, dx dt.$$

We introduce the transversality condition for the adjoint function:

$$(32) \quad \lambda(x, T) = 0 \quad \text{on } \Omega \times \{t = T\}.$$

The adjoint operator L^* and the adjoint PDE, with initial and boundary conditions, are

$$(33) \quad L^* \lambda = -\lambda_t - f'(u^*) \lambda + h^* \lambda - \sum_{i,j=1}^n \left(a_{ij}(x, t) \lambda_{x_j} \right)_{x_i} + \sum_{i=1}^n (b_i(x, t) \lambda)_{x_i}$$

$$L^* \lambda + \mu \lambda = h^* \quad \Omega \times (0, T),$$

$$(34) \quad \frac{\partial \lambda}{\partial \nu} + q \lambda - \sum_{i=1}^n b_i(x, t) \eta_i \lambda = 0 \quad \partial \Omega \times (0, T),$$

$$(35) \quad \lambda = 0 \quad \Omega \times \{t = T\}.$$

Using the sensitivity, ψ , as the test function, we have the weak form of the adjoint.

Definition 1. *The function $\lambda \in V$ with $\lambda_t \in V^*$ is a weak solution to our problem (33)–(35) if:*

$$(36) \quad \int_Q -\lambda_t \phi \, dx dt + \int_Q \mu \lambda \phi \, dx dt - \int_Q (f'(u^*) - h^*) \lambda \phi \, dx dt$$

$$+ \int_Q \sum_{i,j=1}^n a_{ij}(x, t) \lambda_{x_j} \phi_{x_i} \, dx dt$$

$$- \int_Q \sum_{i=1}^n b_i(x, t) \lambda \phi_{x_i} \, dx dt + \int_{\partial \Omega \times (0, T)} q \lambda \phi \, ds dt = \int_Q h^* \phi \, dx dt$$

for all $\phi \in V$ and with $\lambda(x, T) = 0$ for $x \in \Omega$.

Since the adjoint PDE problem is linear in λ , by Evans [2010], an adjoint solution exists.

Theorem 5. *Given an optimal control h^* and the corresponding state solution, u^* , there exists weak solution $\lambda \in V$ satisfying the adjoint system (33)–(35).*

Furthermore, we have the optimality conditions:

$$(37) \quad h^*(x, t) = \begin{cases} h_{max} & : \lambda(x, t) < 1, \\ h_{singular} & : \lambda(x, t) = 1, \\ 0 & : \lambda(x, t) > 1, \end{cases}$$

where $h_{singular}$ can be found from the u^* PDE.

Proof. We will find the control characterization by differentiating the map, $h \rightarrow J(h)$, and using the sensitivity and the adjoint functions. If h^* is optimal, then the difference quotient will be nonpositive since $J(h^*)$ would be the maximum value. So, using the sensitivities, we have

$$\begin{aligned} 0 &\geq \lim_{\epsilon \rightarrow 0^+} \frac{J(h^* + \epsilon l) - J(h^*)}{\epsilon} = \lim_{\epsilon \rightarrow 0^+} \int_Q e^{-\mu t} \frac{1}{\epsilon} [(h^* + \epsilon l)u^\epsilon - h^*u^*] \, dxdt \\ &= \lim_{\epsilon \rightarrow 0^+} \int_Q e^{-\mu t} \left[h^* \left(\frac{u^\epsilon - u^*}{\epsilon} \right) + lu^\epsilon \right] \, dxdt = \int_Q e^{-\mu t} [h^*\psi + lu^*] \, dxdt. \end{aligned}$$

Using the weak formulations for the adjoint and the sensitivity functions, we obtain

$$\begin{aligned} 0 &\geq \int_Q e^{-\mu t} \left[(-\lambda_t + \mu\lambda - f'(u^*)\lambda + h^*\lambda) \psi + \sum_{i,j=1}^n a_{ij}(x, t) \lambda_{x_j} \psi_{x_i} \right. \\ &\quad \left. - \sum_{i=1}^n b_i(x, t) \lambda \psi_{x_i} + lu^* \right] \, dxdt + \int_{\partial\Omega \times (0, T)} e^{-\mu t} q \lambda \psi \, dsdt \\ &= \int_Q e^{-\mu t} \left[\lambda(\psi_t - f'(u^*)\psi + h^*\psi) + \sum_{i,j=1}^n a_{ij}(x, t) \lambda_{x_j} \psi_{x_i} \right. \\ &\quad \left. - \sum_{i=1}^n b_i(x, t) \lambda \psi_{x_i} + lu^* \right] \, dxdt + \int_{\partial\Omega \times (0, T)} e^{-\mu t} q \lambda \psi \, dsdt \\ &= \int_Q e^{-\mu t} [lu^*(1 - \lambda)] \, dxdt. \end{aligned}$$

Our problem is linear in the control, h , and the switching function is $u^*(1 - \lambda)$. Since $u^* \geq 0$ in Q , we investigate the sign of $(1 - \lambda)$. There are three cases:

- (i) On the set $\{(x, t) | h^*(x, t) = h_{max}\}$, any variation, with support on this set, satisfies $l \leq 0$. Then

$$0 \geq \int_Q e^{-\mu t} l(u^*(1 - \lambda)) \, dxdt$$

implies $\lambda \leq 1$ on this set.

- (ii) On the set $\{(x, t) | h^*(x, t) = 0\}$, any variation, with support on this set, satisfies $l \geq 0$. Then

$$0 \geq \int_Q e^{-\mu t} l(u^*(1 - \lambda)) \, dxdt$$

implies $\lambda \geq 1$ on this set.

- (iii) On the set $\{(x, t) | 0 < h^*(x, t) < h_{max}\}$, any variation function, l , with support on this set, can have arbitrary sign. The inequality (37) implies $(1 - \lambda) = 0$ on this set. When $\lambda = 1$ on a set of positive measure, then $\lambda_t = 0$ and $\lambda_{x_i} = 0$ for $i = 1, \dots, n$. Thus our adjoint PDE becomes

$$-f'(u^*) + h^* + \mu + \sum_{i=1}^n (b_i(x, t))_{x_i} = h^*.$$

Using a similar approach as Joshi et al. [2008], we solve for u^* :

$$u^*(x, t) = (f')^{-1}(\mu + \sum_{i=1}^n (b_i(x, t))_{x_i}).$$

We then can solve the state PDE for h^* to find the singular case, $h_{singular}$. We need $(\mu + \sum_{i=1}^n (b_i(x, t))_{x_i})$ to be in the range of (f') . If not, then the singular case would not occur. If this set has measure 0, then we do not need to consider this case.

Thus, these three conditions give us our optimality conditions (37). \square

Remark 2. When $\sum_{i=1}^n (b_i(x, t))_{x_i} = C$, where C is a constant, then we have the expression for $h_{singular}$ at $\lambda = 1$:

$$0 = f(u) - hu = u(g(u) - h),$$

which can be solved for $h_{singular}^*$:

$$h_{singular}^* = g((f')^{-1}(\mu + C)).$$

5. Numerical simulations. Numerical simulations are run to determine approximate solutions to the optimality system (1)–(3), (33)–(35), and (37). For our illustrative examples, we consider the model for fish stock density on a one-dimensional spatial domain of length L , with Robin boundary conditions

$$(38) \quad u_t = (a(x, t)u_x)_x + b(x, t)u_x + f(u) - h(x, t)u,$$

$$(39) \quad \frac{\partial u}{\partial \nu}(x, t) + qu(x, t) = 0,$$

where the diffusion and advection coefficients, $a(x, t)$ and $b(x, t)$, respectively, are positive and can be heterogeneous functions in space and time. We assume the logistic growth function, $f(u) = u(1 - u)$, where u is the stock density in proportion to the carrying capacity K .

The corresponding adjoint equation and optimal control characterization are

$$(40) \quad -\lambda_t - (1 - 2u^*)\lambda + h^*\lambda - (a(x, t)\lambda_x)_x + (b(x, t)\lambda)_x + \mu\lambda = h^*,$$

$$(41) \quad \frac{\partial \lambda}{\partial \nu} + q\lambda - b(x, t)\eta\lambda = 0,$$

and

$$(42) \quad h^*(x, t) = \begin{cases} h_{max} & : \lambda(x, t) < 1, \\ h_{singular} & : \lambda(x, t) = 1, \\ 0 & : \lambda(x, t) > 1, \end{cases}$$

where h^* is the optimal harvest, u^* is the corresponding optimal state.

The forward–backward iterative technique (Lenhart and Workman [2007]) was used to solve the optimality system, which consists of (38)–(39), (40)–(41), and (42). See Hackbusch [1978] for convergence of method. To solve the PDEs, we use an explicit finite difference method with appropriate upwinding schemes for first-order spatial derivatives and a second-order central difference approximation is used for the diffusion terms. A forward Euler method is used for the time derivative. Convergence of the system is checked using relative errors of the optimality system. For numerical simulations, the mesh size was chosen to be $dx = 0.04$ and $dt = \frac{dx^2}{2.5}$ such that, along with the diffusion and advection coefficients, the Courant–Friedrichs–Lewy (CFL) condition for the stability of the system is satisfied.

We chose an initial condition for our fish stock that satisfied both Robin and Dirichlet boundary conditions. The function was chosen so that the stock of fish

TABLE 1. Parameter description, values, and units.

Parameters	Value	Description	Units
L	4	Habitat length	kilometers (km)
T	4	Final time	years (yrs)
μ	0.2	Discount term	1/yr
q	1	Boundary coefficient	1/km
$a(x, t)$	1	Diffusion coefficient	km ² /yr
$b(x, t)$	varied	Advection coefficient	km/yr

would have a bell-shaped curve where most of the stock is concentrated on the middle of the domain:

$$(43) \quad u(x, 0) = \frac{1}{24}x^2(x - L)^2.$$

Parameter values for simulations are listed in Table 1. We consider a spatial domain in terms of kilometers and time in terms of years. Our time scale was chosen such that the population would reach the steady state approximately halfway through the simulation. We set our diffusion coefficient and varied the value of the advection coefficient. The values for our advection coefficient will be chosen in the interval $[0, 1]$. In our numerical simulations, the singular control case never occurred. There was also no evidence of nonuniqueness in the optimal control.

An illustration of the stock density at the initial time with the initial condition, (43), is given in Figure 1, which we will use to compare results with Dirichlet and Robin boundary conditions. When comparing scenarios with Robin boundary conditions, we will use the steady states for the model, with varying levels of exploited initial stock densities. Those steady states were found using different levels of constant harvest on the system. They are visually represented in Figure 1.

5.1. Comparison of boundary conditions. Given the initial condition, (43), we simulated the model without harvest and without advection to investigate the dynamics of the fish stock. Robin boundary conditions allow for the flux across the boundary to be proportional to the stock at the boundary. Dirichlet boundary conditions are lethal to the fish stock at the boundary while Neumann boundary conditions represent a no-flux boundary where the stock cannot leave the boundary. The three cases are shown in the Figure 2.

We compare results with Robin boundary conditions with previous work with Dirichlet boundary conditions (Joshi et al. [2008]), using the initial condition, (43).

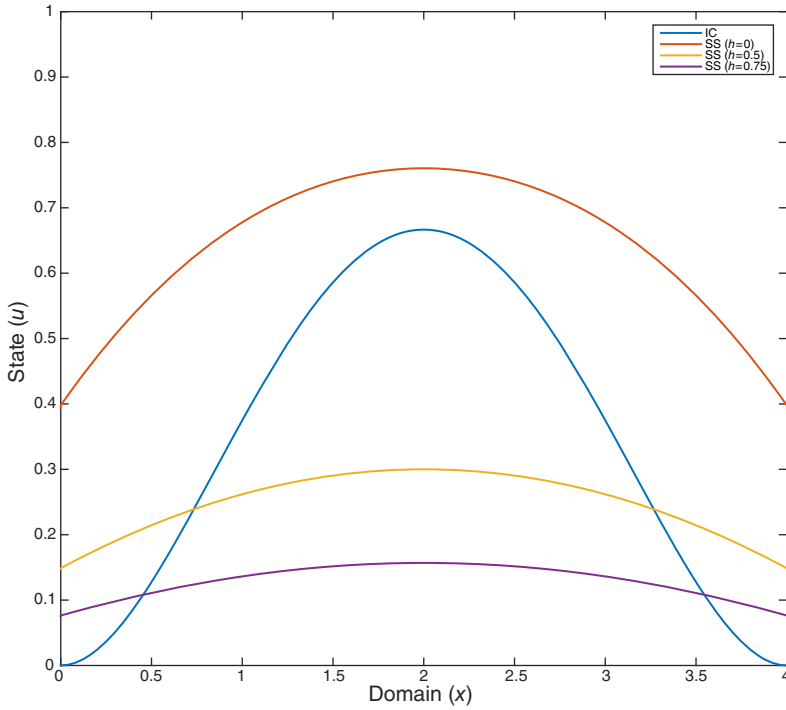


FIGURE 1. Steady states (SS) for varying levels of constant harvest. The initial condition (IC) for stock density used in Dirichlet and Robin boundary condition comparisons is shown in blue.

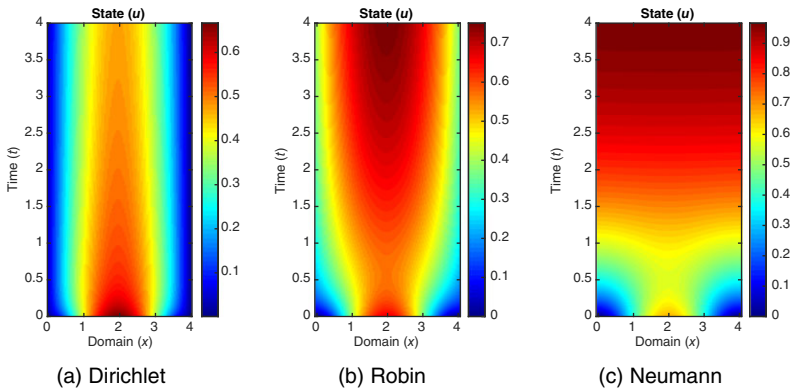


FIGURE 2. Comparison of fish stock dynamics with three different boundary conditions.

TABLE 2. Objective functional values for Dirichlet and Robin boundary condition cases without advection.

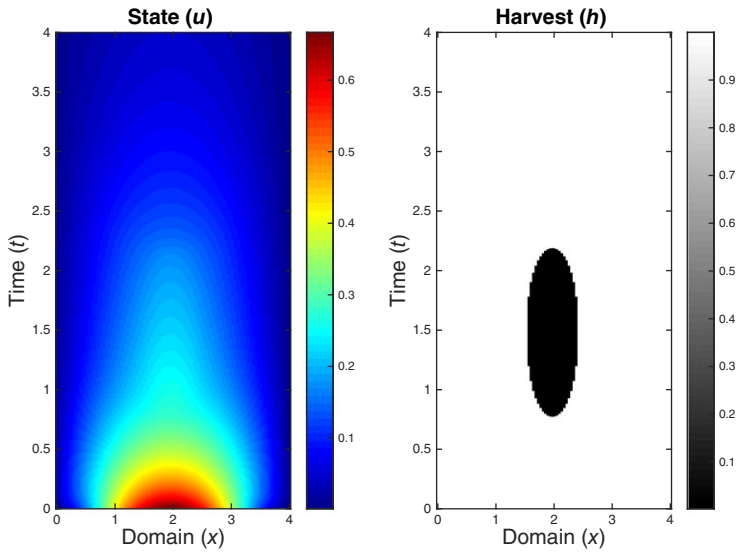
Boundary condition	$J(h^*)$	$J(h_{\max})$
Dirichlet	1.3624	1.3551
Robin	1.9770	1.9143

With Robin boundary conditions, fish stock diffusing to the boundary has less threat of dying as in the Dirichlet boundary case with its lethal boundary. We first compare results without advection ($b(x, t) = 0$). We see in Figure 3a that a reserve exists in the Dirichlet boundary case but is smaller due to the higher chance of the stock reaching the boundary, dying, and no longer being of any value to the stockholder. Due to the conditions of the habitat at the Dirichlet boundary, the projected yield value of the stock is higher, thus the stock is harvested at maximum strength in a larger amount of the habitat than in the Robin boundary case.

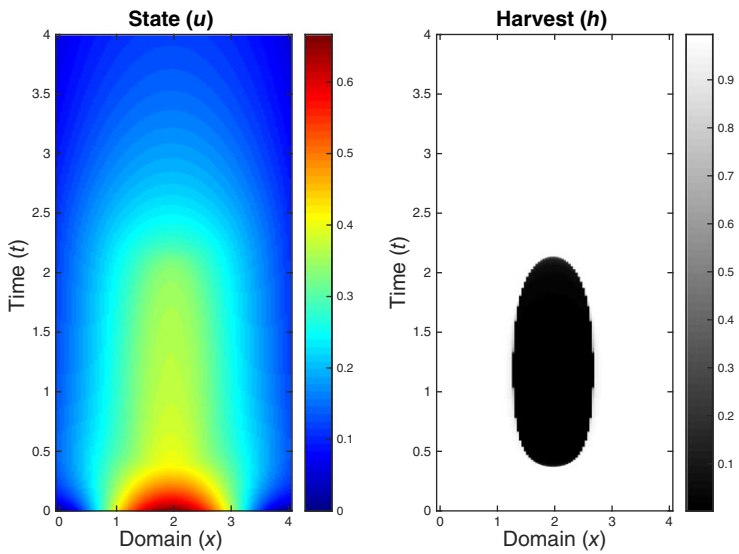
In the Robin boundary condition case, Figure 3b, more of the habitat is kept as a reserve, and for longer time, than in the Dirichlet boundary case since there is less threat of losing stock at the boundary. There are also more fish present in the habitat longer in time as seen in the states in Figure 3. When comparing the objective functional values for both cases, shown in Table 2, notice that, even with the larger reserve, the value of the objective functional in the Robin boundary condition case is higher. We also note that the objective functional values for the optimal strategy are higher than cases where the domain is harvested at the maximum level for the entire time.

Ocean environments are subject to varying currents throughout space and time. In numerical simulations with constant advection, Joshi et al. [2008] concluded that the location of reserves shifted in the opposite direction of advection of the fish stock. Advection acts by pulling the stock in a certain direction and represents currents in the environment. We investigate constant advection throughout space and time, as well as several heterogeneous advection terms. First, we illustrate a constant advection coefficient, $b(x) = 0.5$. We then compare results with heterogeneous advection function coefficients varying in space, using two advection function coefficients, $b(x) = \sin(\frac{\pi x}{4})$ and $b(x) = e^{-0.5x}$. Each represent high advection in certain regions of spatial domain. Finally, we investigate one scenario where the advection function varies in space and time; the spatial domain tries to account for regions of high and low currents that shift over time, with $b(x, t) = \frac{1}{2}(\sin(\pi x + t) + 1)$.

With a constant advection, seen in Figure 4, the location of the reserve shifts in the opposite direction of where advection pulls the stock in both cases. This is because the location farthest from where the stock is moving has the least value to

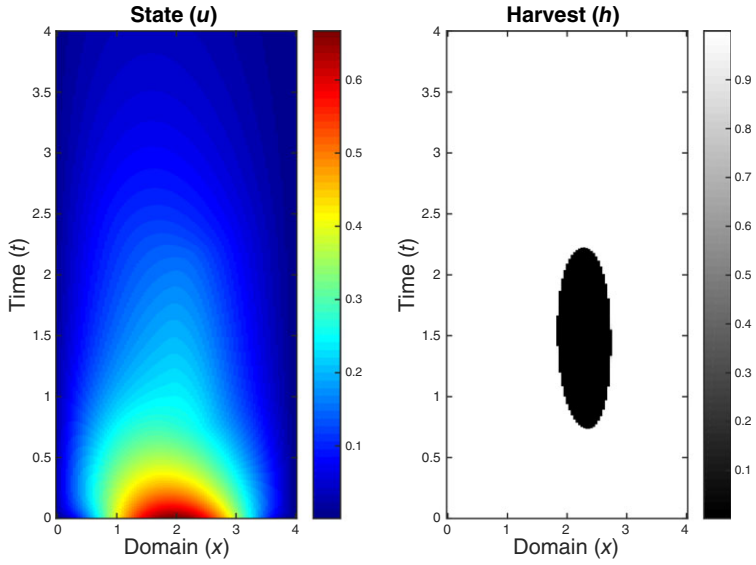


(a) Dirichlet

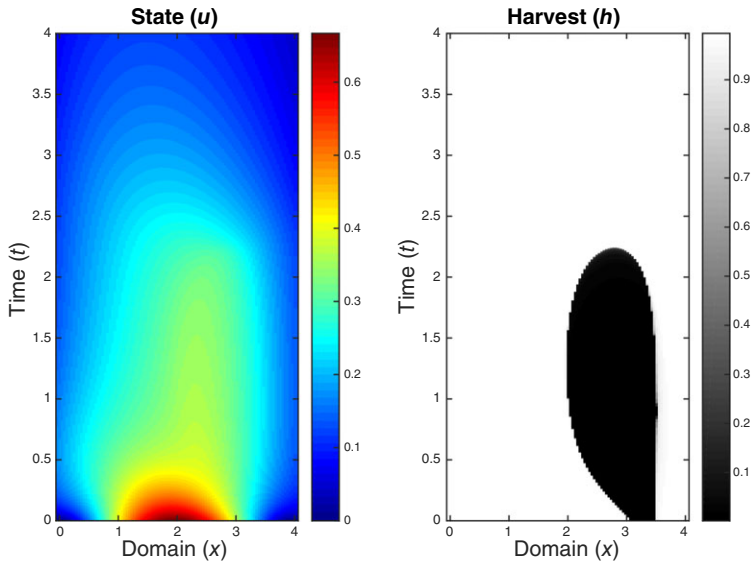


(b) Robin

FIGURE 3. Comparison of stock dynamics and optimal harvesting strategies for Dirichlet and Robin boundary conditions without advection, $b(x, t) = 0$.



(a) Dirichlet



(b) Robin

FIGURE 4. Comparison of stock dynamics and optimal harvesting strategies for Dirichlet and Robin boundary conditions with constant advection, $b(x, t) = 0.5$.

TABLE 3. Objective functional values for Dirichlet and Robin boundary condition cases with varying advection coefficients.

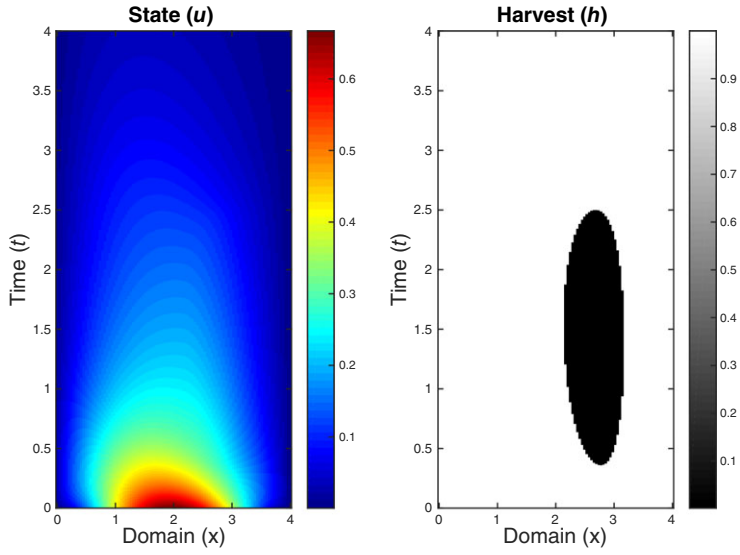
Boundary	$b(x) = 0.5$	$b(x) = \sin(\frac{\pi x}{4})$	$b(x) = e^{-0.5x}$	$b(x, t) = \frac{1}{2}(\sin(\pi x + t) + 1)$
Dirichlet	1.3148	1.2587	1.4756	1.3468
Robin	1.9337	1.9855	2.1501	2.0034

harvest. Stock in this area has less of a chance of being lost at the boundary. In the Dirichlet boundary case, Figure 4a, since stock is being strongly pulled toward a lethal boundary, the reserve is shifted in the opposite direction and the reserve is smaller than in the cases without advection. This is due to advection raising the risk of stock dying on one side of the boundary. In the Robin boundary case, Figure 4b, since the boundary is not necessarily lethal, it is not as valuable to harvest at maximum strength in as large of an area as the Dirichlet boundary case. A larger reserve exists and opens sooner because there is a smaller chance that stock in that area of the habitat will be lost.

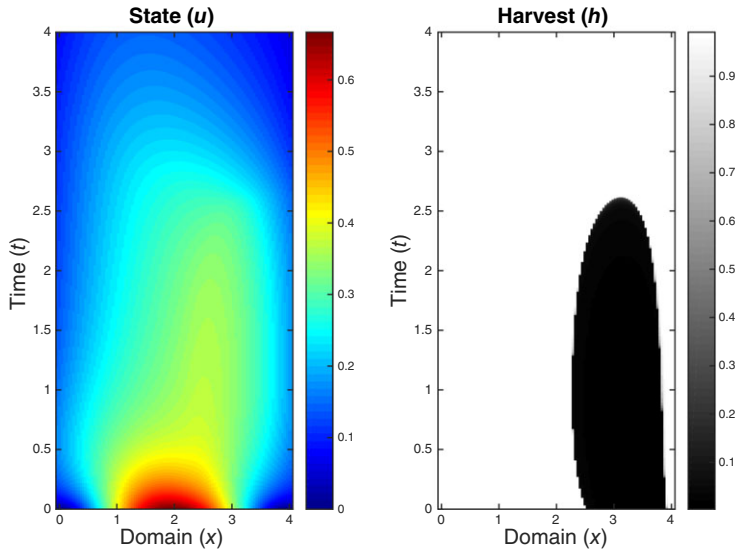
Results on how advection function coefficients, varying in space, affect the harvest strategy are found in Figures 5 and 6. Table 3 compares the objective functional values for the Dirichlet and Robin boundary condition cases. Despite larger reserves forming, the objective functional values for the Robin boundary condition cases are always higher than the Dirichlet boundary cases.

In the cases where the advection coefficient is heterogeneous across the spatial domain, we see similar results as in the constant advection cases. The reserve is still shifted in the direction opposite from where the stock is being pulled, however, the shape and length of the reserves vary, especially seen in Figure 5. In this case, there is a strong advection term in the center of the habitat, where the fish stock is initially concentrated. The reserve begins much earlier and is shifted further than other cases. Since advection is strong in the center of the domain, there is a larger risk of stock being pulled to the boundary and lost so it becomes more profitable to harvest. Again, we see the reserve opening earlier and persisting longer in the Robin boundary case because the stock is less valuable to harvest since there is less chance of being pulled to the boundary and lost.

In Figure 6, the result is more similar to the constant advection case from Figure 4. In this case, the advection is strongest on one side of the habitat. The reserve in the Robin boundary case is wider, opens earlier, and shifted more than in Dirichlet boundary case. This is due to areas where advection is highest being the most valuable to harvest because of the chance for stock to be lost at the boundary. The stock in other parts of the domain, where the current is less strong, is less valuable to harvest, which is a reason why the reserve forms here and is larger. Another

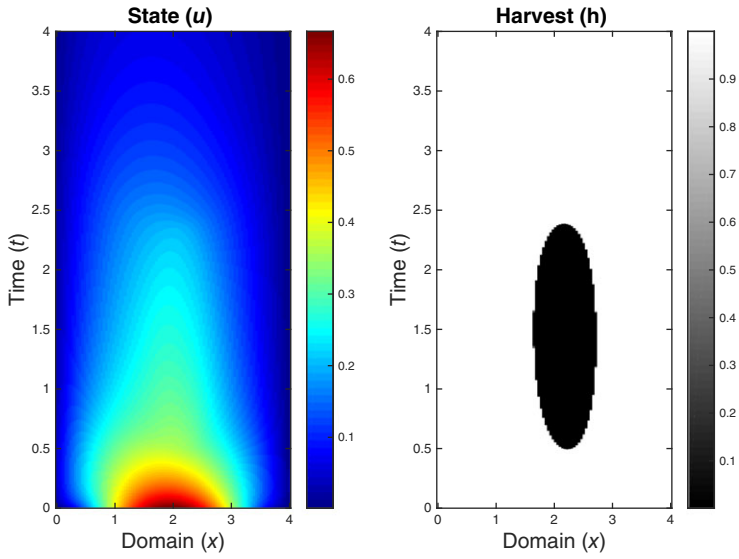


(a) Dirichlet

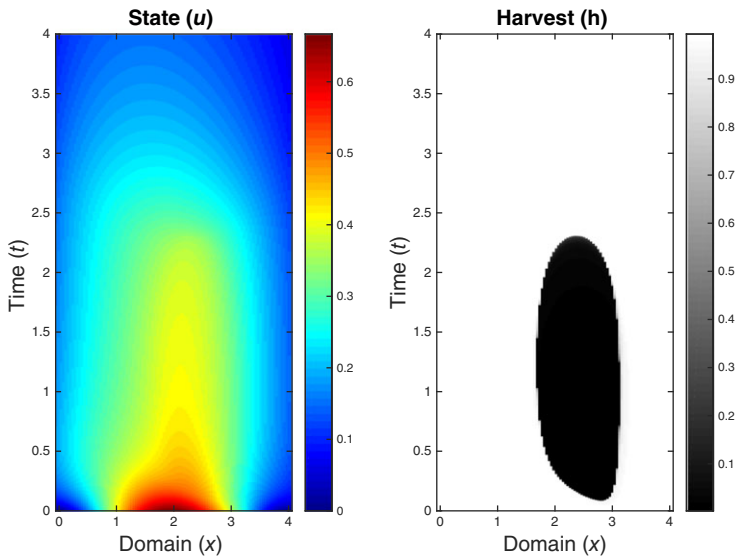


(b) Robin

FIGURE 5. Comparison of stock dynamics and optimal harvesting strategies for Dirichlet and Robin boundary conditions with advection, $b(x) = \sin(\frac{\pi x}{4})$.



(a) Dirichlet



(b) Robin

FIGURE 6. Comparison of stock dynamics and optimal harvesting strategies for Dirichlet and Robin boundary conditions with advection, $b(x) = e^{-0.5x}$.

thing to note is that the reserve does not hit either edge of the habitat in any of the cases. Although the advection is strongly pulling the stock to one side of the habitat, there is still diffusion distributing the stock across the domain and there is still stock moving to both ends of the habitat. Thus, it is advantageous to harvest in all areas closest to the boundary.

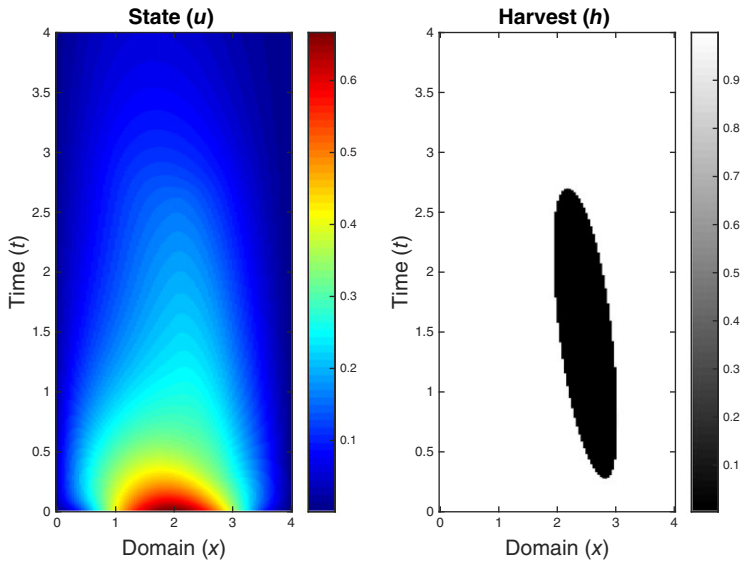
Figure 7 illustrates when the advection coefficient changes in both space and time. Notice, for both cases, the similar shift in the direction the reserve forms that is dependent on the direction the current moves. Again, as previously seen, a larger reserve is formed in the Robin boundary condition case than in Dirichlet boundary case. When comparing the harvesting strategies with the advection function, $b(x, t)$, it is interesting to note where the reserve forms. The reserve in both cases forms next to an area of the domain with the highest advection values, always on the side opposite of where stock is being pulled.

5.2. Comparison of varying scenarios with Robin boundary conditions.

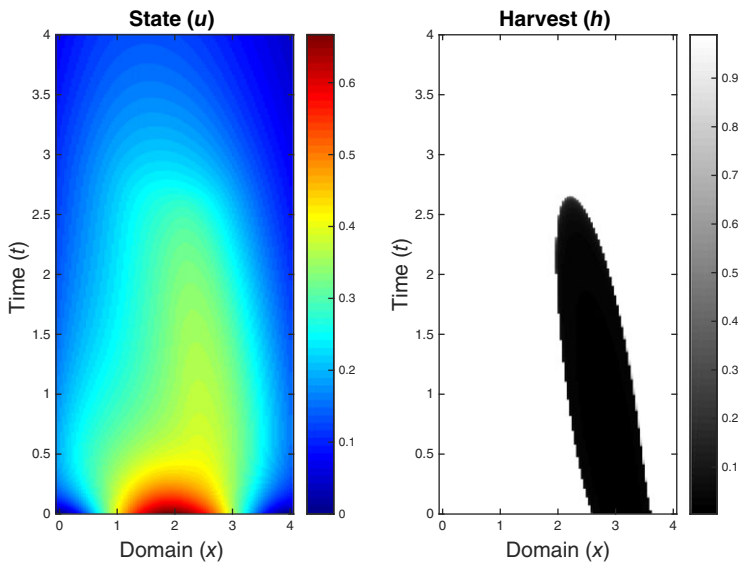
As we saw in the previous subsection, there is a definite difference when the domain incorporates Dirichlet or Robin boundary conditions. Although reserves were always part of the optimal harvesting strategy, the size, shape, and timing are affected by both the boundary conditions and varying advection function coefficients. In this section, we will investigate more closely the domain with Robin boundary conditions and how different scenarios affect the optimal harvesting strategies. We begin with optimal harvesting results for constant advection coefficients, $b(x)$, with varying constant values on the interval $[0, 1]$, found in Figure 8. We then compare the optimal harvesting results with advection coefficients that are heterogenous in space or time, bounded on the interval $[0, 1]$. In these scenarios, we use the steady state of unexploited fish stock without harvest as our initial condition (see Figure 1). The results are shown in Figure 9.

As the constant advection coefficient increases, we see an increase in the shift of the reserve in the opposite direction of the pull. In the cases with a heterogenous advection coefficient, Figure 9, there is more variation in the shape of the reserve. The location of strong currents in a domain affects harvest strategies. Stronger currents through the center of a domain affect a larger portion of the stock than if only concentrated on one side of the domain or constant throughout, thus altering where and when reserves develop and their size. Again, as the advection function varies in time (Figure 9 d), a reserve forms to the right of highest advection areas and the reserve follows the movement of advection, forming on a diagonal. An understanding of ocean currents within a fishery, as well as their variation in time, appears necessary in determining where reserves should be implemented.

5.3. Optimal harvesting strategy results for an initially unexploited and exploited stock. In previous results, simulations were run using the steady



(a) Dirichlet



(b) Robin

FIGURE 7. Comparison of stock dynamics and optimal harvesting strategies for Dirichlet and Robin boundary conditions with advection, $b(x, t) = \frac{1}{2}(\sin(\pi x + t) + 1)$.

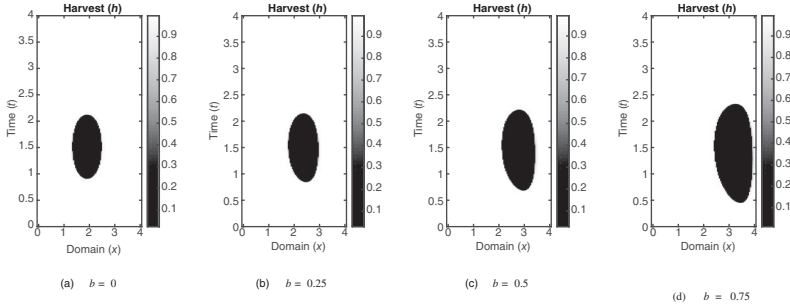


FIGURE 8. Comparison of optimal harvesting strategies for Robin boundary conditions with varying constant advection coefficients.

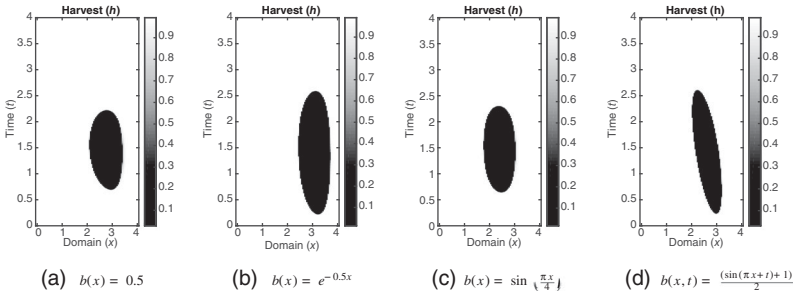


FIGURE 9. Comparison of optimal harvesting strategies for Robin boundary conditions with varying advection function coefficients.

state of an unexploited fish stock. Due to current fishing practices, many stocks are either exploited or overexploited. In this subsection, we investigate optimal harvesting strategies with different levels of fish stock at the initial time, when the stock is initially unexploited, exploited, or overexploited. Figure 1 shows the steady states considered, with varying harvest values. Figure 10 shows varying results with different levels of stock at the initial time.

With an initially overexploited fish stock, there is a need for a reserve starting at $t = 0$ to rebuild the stock. Once the stock recovers, the reserve decreases in size, eventually closing, and maximum harvest persists for the remaining time. This makes sense in cases when trying to maximize yield. It is important for stock to grow before depleting the stock again. The practicality of its implementation is debatable since, depending on the level of overexploitation, large portions of the habitat would be closed to fishing. The effect on the fishing industry would be drastic in the short term.

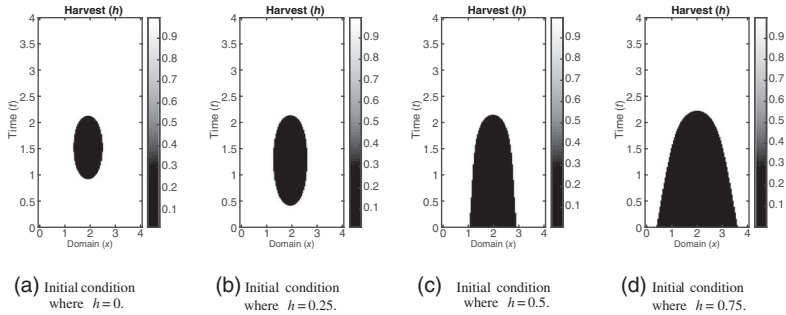


FIGURE 10. Comparison of optimal harvesting strategies for Robin boundary conditions for various exploited initial stock densities. The initial conditions for (a) were set as the equilibrium of a previously unexploited stock. The initial conditions for each panel from left to right, (b)–(d) were chosen to simulate an increasingly overexploited stock.

TABLE 4. Comparison of objective functional values for the optimal harvest strategy and an approximation to that harvesting strategy with varying advection coefficients.

Advection	$J(h^*)$	$J(h_{\text{approx}})$
$b(x, t) = 0$	2.8522	2.8504
$b(x, t) = 0.75$	2.7414	2.7399
$b(x) = \sin\left(\frac{\pi x}{4}\right)$	2.8400	2.8387

5.4. Approximations of optimal harvesting strategy results. In the implementation of a harvesting strategy, there is debate on the feasibility of adjusting the effort through space and time. In this section, we compare the optimal harvesting strategy results from the previous sections with an approximation of the harvesting strategy that is either constant in space or in both space and time. We compare the objective functional values for both to determine how close the approximation is to the optimal result.

In the previous section, we found the optimal harvesting strategies for Robin boundary conditions given certain scenarios. We investigate the scenario without advection and then two with advection coefficients. The results for the case without advection are found in Figure 11 and Table 4. We investigate the constant advection coefficient of $b(x) = 0.75$ and the heterogeneous advection coefficient, $b(x) = \sin\left(\frac{\pi x}{4}\right)$. The results are shown in Figures 12 and 13, and Table 4, respectively. In Figures 11–13, in the approximation, the reserve was chosen to be rectangular and to be close to optimal reserve location.

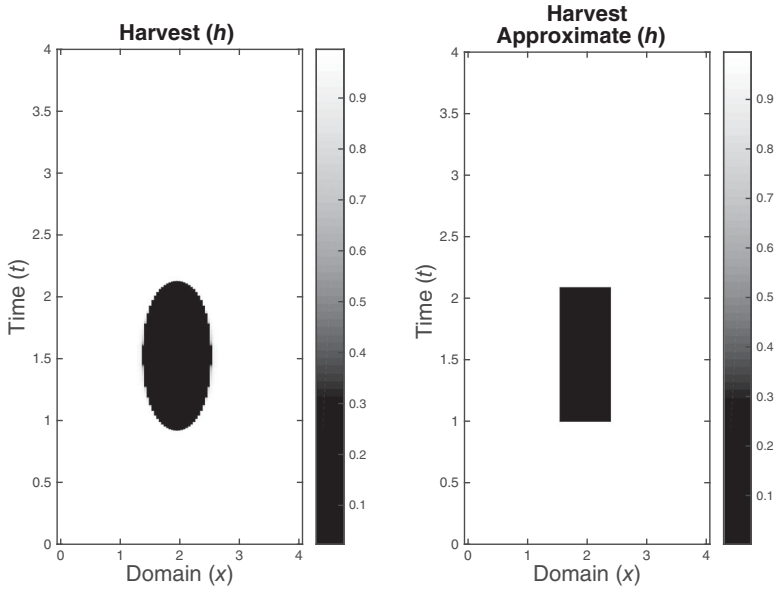


FIGURE 11. Comparison of optimal harvesting strategy for Robin boundary conditions and an approximation of that harvesting strategy, without advection.

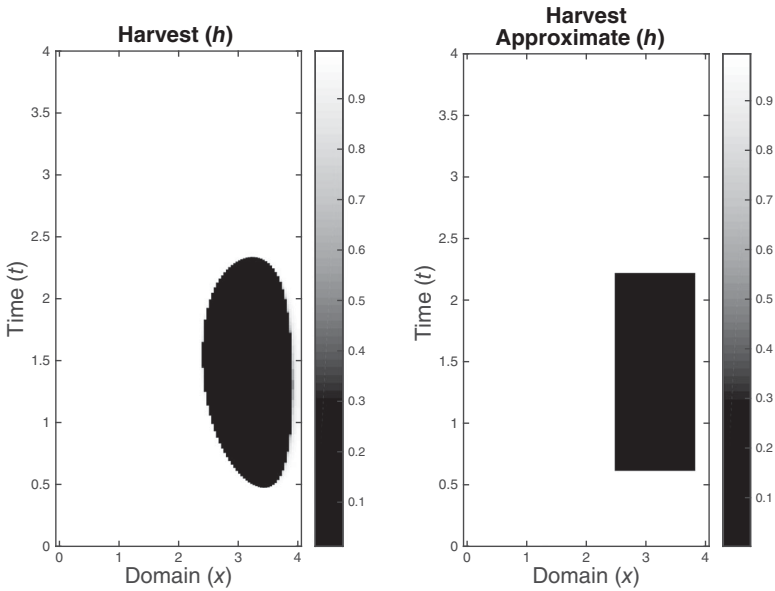


FIGURE 12. Comparison of optimal harvesting strategy for Robin boundary conditions and an approximation of that harvesting strategy, with constant advection, $b(x, t) = 0.75$.

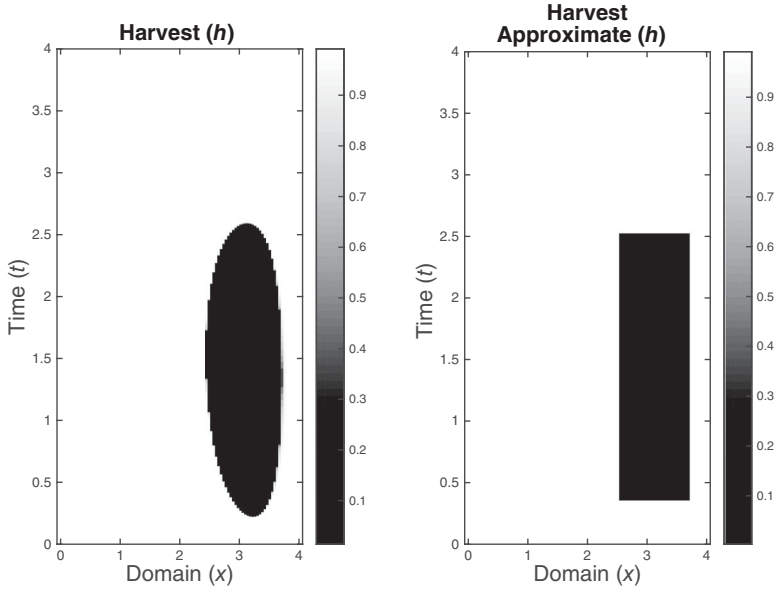


FIGURE 13. Comparison of optimal harvesting strategy for Robin boundary conditions and an approximation of that harvesting strategy, with advection function coefficient, $b(x) = \sin(\frac{\pi x}{4})$.

In each of the cases, harvest approximations can be found that are close to the optimal harvest strategies found through the simulations. The approximations were found by choosing finite space and time intervals in locations and sizes that best estimate the optimal harvesting strategy. In all the cases, as seen by the objective functional values in Table 4, the approximations are obviously less than the optimal but there is evidence to believe that if you approximated the harvest, the resulting objective functional would be very close. The largest difference between the approximate and actual optimal objective functional values is less than 0.5%. The approximations may be more realistic in regards to actual implementation of reserves because it is easier to form reserves that are constant in space and open/close in time.

Another option to consider is when the harvest does not vary in time. In Figures 14 and 15, with Table 5, we compare the results with the optimal harvesting strategy in the dynamic harvest case with no advection, using a narrower reserve as approximation. We also include the objective functional values for the case with maximum harvest on the entire domain in Table 5 for comparison. When the domain is harvested at the maximum for the entire time, we see sub-optimal results as expected, with an objective functional value lower than in the optimal harvest case (approximately 1% lower). When considering a harvest not

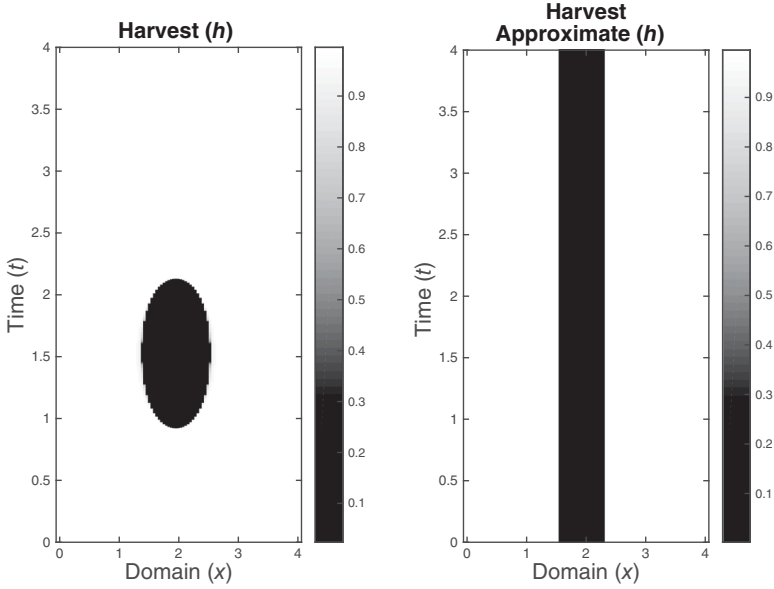


FIGURE 14. Comparison of optimal harvesting strategy for Robin boundary conditions and an approximation of that harvesting strategy, not varying in time, without advection.

TABLE 5. Comparison of objective functional values for the optimal harvest strategy, an approximation to that harvesting strategy, and maximum harvest on entire domain, without variation over time and without advection.

$J(h^*)$	$J(h_{\text{approx}})$	$J(h_{\text{max}})$
2.8522	2.7259	2.8310

varying in time, the objective functional value is still lower than in the optimal case, seen in Table 5. In this approximate case, there are higher stock levels at the final time, seen in Figure 15. However, when trying to maximize yield only, it is not as close to optimal as other approximations (approximately 5% lower). This points to evidence that time managed reserves are important when considering reserves. More work needs to be done in this area, such as investigating harvest dependent only on space or time and determining the optimal harvesting strategies associated with them, rather than just using these approximations of the optimal.

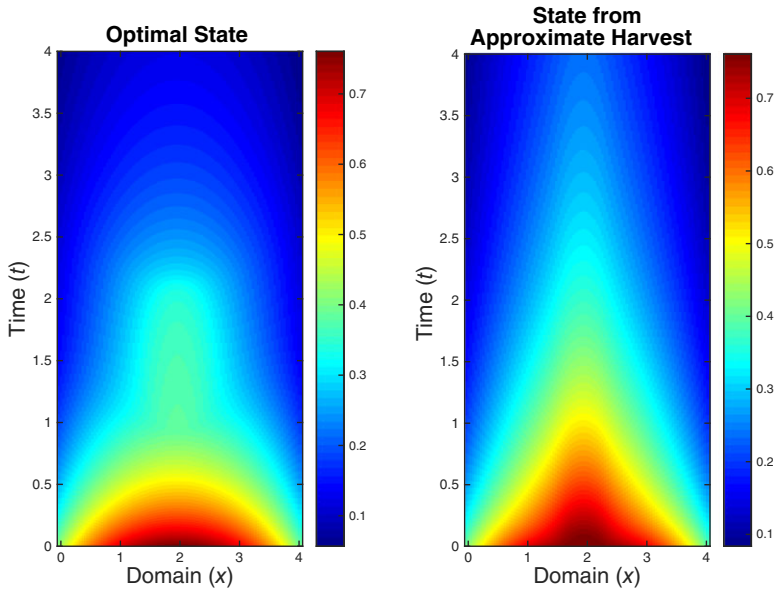


FIGURE 15. Comparison of the corresponding state solution for the optimal harvesting strategy and the approximation to that harvesting strategy, not varying in time, without advection.

6. Conclusions. Our work highlights the importance of appropriate boundary conditions, corresponding to specific fishing scenarios, in finding harvest management strategies. A more realistic boundary condition produces different harvesting results than previous results with Dirichlet boundary conditions. Although there may be scenarios when lethal, Dirichlet boundaries should be used, when considering open ocean fisheries, the implementation of a nonlethal boundary, using Robin boundary conditions, produced results with larger yield values as well as reserve sizes.

We further investigated how the interplay between Robin boundary conditions and advection within the domain affected harvesting strategies. Similar to previous work of Joshi et al. [2008], a reserve opens and is shifted in the opposite direction from that toward which the stock is being pulled. However, the reserves are larger than in previous work. When we investigated advection functions that varied in space or time, there was even more disparity among the size and shape of reserves. When the advection shifted in time, a reserve forms that followed a similar directional pattern as the advection. We also compared harvesting strategies for scenarios when the stock size is initially unexploited, exploited, and overexploited. We saw that when the stock is initially overexploited, reserves are opened immediately

and cover most of the domain. Once the stock has time to recover, the reserve closes and the domain is harvested at maximum levels the rest of the time.

When considering the implementation of these reserves, we decided to approximate the optimal harvest strategies using reserves that, once open, do not vary in space. We saw that approximate reserves produced suboptimal objective values but the values were relatively close (less than 0.5% difference). In the case where we compared the optimal harvest strategy with an approximate harvest strategy with reserves not varying in time, there was a significant difference in objective values and the stock levels at the final time (objective values approximately 5% less). Using spatial boundaries that are constant in time (reserve is rectangular in space and time) and restricting the length of time to impose a reserve are realistic and can achieve near optimal results.

We saw that currents varying through space and time affected harvesting strategies. There is evidence that a better understanding of ocean currents within a habitat and how they vary through time is important when determining the location and time of a reserve, as well as its size. With the added complexity to the domain, we believe harvesting strategies will also be affected.

Acknowledgments. Kelly's and Lenhart's work was partially supported by the National Institute for Mathematical and Biological Synthesis (NIMBioS) at The University of Tennessee, Knoxville, sponsored by the National Science Foundation (NSF Grant #EF-0832858).

REFERENCES

- G.M. Brown and J. Roughgarden [1997], *A Metapopulation Model with Private Property and a Common Pool*, *Ecol. Econ.* **30**, 293–299.
- C.W. Clark [1985], *Bioeconomic Modelling and Fisheries Management*, Wiley, New York.
- C.W. Clark [1990], *Mathematical Bioeconomics: The Optimal Management of Renewable Resources* (2nd edition), Wiley, New York.
- C.W. Clark [2006], *The Worldwide Crisis in Fisheries*, Cambridge University Press, New York.
- W. Ding and S. Lenhart [2009], *Optimal Harvesting of a Spatially Explicit Fishery Model*, *Nat. Resour. Model.* **22**(2), 173–211.
- L. Evans [2010], *Partial Differential Equations* (2nd edition), American Mathematical Society, Providence, Rhode Island.
- W. Fagan, R.S. Cantrell, and C. Cosner [1999], *How Habitat Edges Change Species Interactions*, *Am. Nat.* **153**(2), 165–182.
- W. Hackbusch [1978], *A Numerical Method for Solving Parabolic Equations with Opposite Orientations*, *Computing* **20**(3), 229–240.
- G.E. Herrera and S. Lenhart [2010], *Spatial Optimal Control of Renewable Resource Stocks*, in *Spatial Ecology*, Mathematical and Computational Biology Series, Chapman & Hall, CRC, Singapore, Boca Raton, Florida. pp. 343–357.
- R. Hilborn [2012], *Overfishing: What Everyone Needs to Know*, Oxford University Press, Oxford.

- H. Joshi, G. Herrera, S. Lenhart, and M. Neubert [2008], *Optimal Dynamic Harvest of a Mobile Renewable Resource*, Nat. Resour. Model. **10**(40), 322–343.
- P. De Leenheer [2014], *Optimal Placement of Marine Protected Areas: A Trade-Off between Fisheries Goals and Conservation Efforts*, IEEE Trans. Automat. Contr. **59**(6), 1583–1587.
- S. Lenhart, M. Liang, and V. Protopopescu [1999], *Optimal Control of Boundary Habitat Hostility for Interacting Species*, Math. Methods Appl. Sci. **22**, 1061–1077.
- S. Lenhart and D.G. Wilson [1993], *Optimal Control of a Heat Transfer Problem with Convective Boundary Condition*, J. Optim. Theory Appl. **79**(3), 581–597.
- S. Lenhart and J.T. Workman [2007], *Optimal Control Applied to Biological Models*, Chapman & Hall, London.
- G.M. Lieberman [1996], *Second Order Parabolic Differential Equations*, World Scientific Publishing Company, Singapore.
- M. Neubert [2003], *Marine Reserves and Optimal Harvesting*, Ecol. Lett. **6**, 843–849.
- J.N. Sanchirico and J.E. Wilen [1999], *Bioeconomics of Spatial Exploitation in a Patchy Environment*, J. Environ. Econ. Manage. **37**, 129–150.
- J.N. Sanchirico and J.E. Wilen [2001], *A Bioeconomic Model of Marine Reserve Creation*, J. Environ. Econ. Manage. **42**, 257–276.
- J. Simon [1987], *Compact Sets in the Space $L^p(0, T; B)$* , Ann. di Mate. Pura ed Appl. **CXLVI**(IV), 65–96.
- C. Toropova, I. Meliane, D. Laffoley, E. Matthews, and M. Spalding, editors. [2010], *Global Ocean Protection: Present Status and Future Possibilities*, IUCN, The Nature Conservancy, UNEP-WCMC, UNEP, UNU-IAS, Agence des aires marines protégées, Gland, Switzerland, Arlington, USA, Cambridge, UK, Nairobi, Kenya, Tokyo, Japan, Brest, France.
- G.N. Tuck and H.P. Possingham [2000], *Marine Protected Areas for Spatially Structured Exploited Stocks*, Mar. Ecol. Prog. Ser. **192**, 89–101.
- C.J. Walters and S.J.D. Martell [2004], *Fisheries Ecology and Management*, Princeton University Press, Princeton, New Jersey.